Myocardial Morphological Characteristics and Proarrhythmic Substrate in the Rat Model of Heart Failure Due to Chronic Volume Overload

JIRI BENES JR.,[1,2,3]* VOJTECH MELENOVSKY,[4,5] PETRA SKAROUPKOVA,[5,6] JANA POSPISILOVA,[7] JIRI PETRAK,[7] LUDEK CERVENKA,[5,6] AND DAVID SEDMERA[1,2]

[1]Charles University in Prague, First Faculty of Medicine, Institute of Anatomy, U nemocnice 3, 12800 Prague 2, Czech Republic

[2]Institute of Physiology, Department of Cardiovascular Morphogenesis, Academy of Sciences of the Czech Republic, Videnska 1083, 14220 Prague 4, Czech Republic

[3]Department of Radiology of the First Faculty of Medicine and General Teaching Hospital, Charles University in Prague, First Faculty of Medicine, U Nemocnice 2, Prague 2, Czech Republic

[4]Department of Cardiology, Institute of Clinical and Experimental Medicine-IKEM, Videnska 1958/9, 14021 Prague 4, Czech Republic

[5]Center for Cardiovascular Research, Institute of Clinical and Experimental Medicine-IKEM, Videnska 1958/9, 14021 Prague 4, Czech Republic

[6]Center of Experimental Medicine, Institute of Clinical and Experimental Medicine-IKEM, Videnska 1958/9, 14021 Prague 4, Czech Republic

[7]Charles University in Prague, First Faculty of Medicine, Institute of Pathological Physiology, U nemocnice 5, 12800 Prague 2, Czech Republic

ABSTRACT

Chronic volume overload leads to cardiac hypertrophy and later to heart failure (HF), which are both associated with increased risk of cardiac arrhythmias. The goal of this study was to describe changes in myocardial morphology and to characterize arrhythmogenic substrate in rat model of developing HF due to volume overload. An arteriovenous fistula (AVF) was created in male Wistar rats between the inferior vena cava and abdominal aorta using needle technique. Myocardial morphology, tissue fibrosis, and connexin43 distribution, localization and phosphorylation were examined using confocal microscopy and Western blotting in the stage of compensated hypertrophy (11 weeks), and decompensated HF (21 weeks). Heart to body weight (BW) ratio was 89% and 133% higher in AVF rats at 11 and 21 weeks, respectively. At 21 weeks but not 11 weeks, AVF rats had pulmonary congestion (increased lung to BW ratio) indicating presence of decompensated HF. The myocytes in left ventricular midmyocardium were significantly thicker (+8% and +45%) and longer (+88% and +97%). Despite extensive hypertrophy, there was no excessive fibrosis in the AVF ventricles. Distribution and localization of connexin43 were similar between groups, but its phosphorylation was significantly lower in AVF hearts at 21st week, but not 11th week, suggesting that HF,

Grant sponsor: Ministry of Education, Youth and Sports; Grant numbers: VZ 0021620806, 1M0510, 1M0538, LC06044 and 1M6798582302; Grant sponsor: Academy of Sciences of the Czech Republic; Grant number: AV0Z50110509; Grant sponsor: Grant Agency of the Czech Republic; Grant numbers: 304/08/0615 and 305/09/1390; Grant sponsor: Ministry of Health of the Czech Republic; Grant numbers: MZO-00023001 and NS10497-3/2009.

*Correspondence to: Jiri Benes Jr., Institute of Anatomy, U nemocnice 3, 12800, Prague 2, Czech Republic.
E-mail: jiri.benes2@lf1.cuni.cz

Received 15 January 2010; Accepted 9 September 2010
DOI 10.1002/ar.21280
Published online 2 November 2010 in Wiley Online Library (wileyonlinelibrary.com).

rather than hypertrophy contributes to the connexin43 hypophosphorylation. In conclusion, volume overload leads to extensive eccentric hypertrophy, but not to myocardial fibrosis. Increased vulnerability to arrhythmia in this HF model is possibly related to gap junction remodeling with hypophosphorylation of connexin43. Anat Rec, 294:102–111, 2011. © 2010 Wiley-Liss, Inc.

Key words: cardiac hypertrophy; heart failure; connexin43; rat

The increase in volume loading of the heart due to valve insufficiency or arteriovenous fistula (AVF) causes dilation of cardiac chambers and cardiac hypertrophy (Ford, 1976). It is believed that this process is due to cardiomyocyte elongation and hypertrophy that compensate volume overload and normalize wall stress (Grossman et al., 1975). Despite cardiac output being often increased (such as in the case of chronic arteriovenous fistula–AVF), substantial part of stroke volume is shunted or recirculated and is not contributing to systemic perfusion. Diminished systemic perfusion leads to redistribution of cardiac output and neurohumoral activation. When compensatory mechanisms become inadequate, overt heart failure (HF) develops (Hood et al., 1968) in a way similar to other models of LV hypertrophy-HF transition (Hatt et al., 1979; Legault et al., 1990; Ruzicka et al., 1993; Ryan et al., 2007).

Regardless its etiology, cardiac hypertrophy is associated with increased incidence of potentially life-threatening ventricular arrhythmias (Artham et al., 2009) and is one of the strongest risk factors for sudden cardiac death (Haider et al., 1998). The mechanisms of arrhythmias in eccentric hypertrophy due to volume overload are known less than in cardiac hypertrophy due to pressure overload or chronic myocardial infarction. Arrhythmogenesis is often linked to increased electrical heterogeneity of myocardial tissue and slowed impulse conduction (Shah et al., 2005). The involved mechanisms consist of myocardial fibrosis, changes in cell and tissue architecture, membrane excitability, and alterations of gap-junctional coupling (Libby et al., 2008). Gap junctions are required for electrical impulse propagation and synchronous contraction in the healthy heart and their alterations might contribute to abnormal conduction and thus be a substrate for arrhythmia (von Olshausen et al., 1983; Kligfield et al., 1987; Kostin et al., 2003; Wiegerinck et al., 2008). The main protein forming gap junctions in rat ventricular myocardium is connexin43 (Sohl and Willecke, 2004). Changes in amount and in localization of connexin43 have been reported in the diseased myocardium (Severs et al., 2004). Some of the previous studies demonstrated a reduction in connexin43 levels in left ventricles of transplant patients with end-stage HF (Dupont et al., 2001). Lateralization of connexin43 from intercalated discs to lateral membrane of myocytes occurs in experimentally induced hypertrophy of right and left ventricle of the rat (Uzzaman et al., 2000; Emdad et al., 2001). Apart from alterations in connexin43 levels, the dephosphorylation of connexin43 was described during several pathological states, including myocardial ischemia (Beardslee et al., 2000; Burstein et al., 2009). Taking all this into an account, new antiarrhythmic drugs targeting function of gap junctions are developed, with rotigaptide, a selective gap junction modifier, as an example (Haugan et al., 2006).

In our study, HF in rats was induced by AVF. Similar volume overload HF models were created also by other groups in dogs (Legault et al., 1990) and rats (Hatt et al., 1979; Ruzicka et al., 1993; Ryan et al., 2007). However, no previous study characterized cardiac morphology at two distinct phases of HF development. The main purpose of this study was thus to provide morphological characteristics of the AVF experimental rat HF model induced by volume overload with a focus on abnormalities in myocardial tissue potentially contributing to arrhythmogenesis, such as fibrosis and connexin43 distribution.

MATERIAL AND METHODS

Animals

The rats were kept in air-conditioned animal facility on a 12-hr/12-hr light/dark cycle. Throughout the experiments the rats were fed a normal salt, normal protein diet (0.45% NaCl, 19−21% protein) produced by SEMED (Prague, Czech Republic) and had free access to tap water. The rats were weighted weekly. Studies were made according to Animal Protection Law of the Czech Republic (311/1997) and were approved by the Ethic Committee of the Institute of Clinical and Experimental Medicine (Prague, Czech Republic).

Male Wistar rats weighting 300−350 g were used for this study and the changes were evaluated in two intervals following the experimental procedure, after 11 and 21 weeks. Some of the animals died after the surgery, this early mortality ($\leq$7 days) occurred mostly within the first 48 hr and was about 13%. Another 5% of animals with AVF died prior to the end of experiment. All animals that died during the course of experiment were excluded from the study. Some of the animals showed milder signs of incipient HF (lethargy, difficult breathing, cyanosis, piloerection), 65% after 11 weeks and 80% after 21 weeks of volume overload. During hemodynamic measurements of LV intraventricular pressure with 2F Millar catheter (data not shown), we observed in ACF rats frequent nonsustained polytopic ventricular ectopy. Approximately in 10% of ACF rats, these manipulations led to sustained ventricular tachycardia degenerating into ventricular fibrillation (VF). In contrast, no complex ectopy or VF was observed in control rats. For quantitative analysis we used seven AVF rats that were sacrificed 11 weeks after the surgery (plus six sham-operated controls at this time point) and seven AVF rats sacrificed

TABLE 1. Changes in weight of internal organs of AVF and Sham-operated rats

Changes at the organ level								
	11 weeks				21 weeks			
Weight (g)	AVF (n = 7)	Sham (n = 6)	Difference	Statistics (t = test)	AVF (n = 7)	Sham (n = 8)	Difference	Statistic s (t-test)
Body	482 ± 33	465 ± 17	+ 3.5%	$P = 0.289$	500 ± 43	487 ± 42	+ 2.6%	P= 0 .597
Heart	2.52 ± 0.32	1.29 ± 0.09	+ 95.7%	$\mathbf{P = 1 \times 10^{-6}}$	2.52 ± 0.34	1.05 ± 0.08	+ 140%	$\mathbf{P = 6 \times 10^{-7}}$
Ventricles	2.05 ± 0.29	1.04 ± 0.08	+ 96.2%	$\mathbf{P = 6 \times 10^{-6}}$	2.02 ± 0.27	0.91 ± 0.06	+ 123%	$\mathbf{P = 7 \times 10^{-7}}$
Atria	0.47 ± 0.10	0.24 ± 0.05	+ 94%	$\mathbf{P = 3 \times 10^{-6}}$	0.49 ± 0.14	0.14 ± 0.02	+ 246%	$\mathbf{P = 1 \times 10^{-4}}$
Lungs	2.07 ± 0.32	1.64 ± 0.19	+ 26.2%	$\mathbf{P = 0.014}$	2.7 ± 0.56	1.68 ± 0.27	+ 61.3%	$\mathbf{P = 0.002}$
Liver	15.30 ± 2.80	15.02 ± 1.67	+ 1.8%	$P = 0.838$	15.88 ± 2.65	14.25 ± 1.10	+ 11.4%	$P = 0.189$
Kidneys	1.34 ± 0.12	1.44 ± 0.11	−7.1%	$P = 0.226$	1.24 ± 0.10	1.27 ± 0.10	−2.25%	$P = 0.481$
HBWR	5.23 ± 0.54	2.77 ± 0.17	+ 88.9%	$\mathbf{P = 4 \times 10^{-7}}$	5.02 ± 0.51	2.16 ± 0.11	+ 133%	$\mathbf{P = 4 \times 10^{-8}}$

HBWR, heart to body weight ratio.
Data are presented as mean ± SD.

21 weeks after the surgery (plus eight sham-operated controls).

Aortocaval Shunt

Aortocaval fistula was created by the method described by Garcia and Diebold (1990). On the day of surgery, anesthesia was induced by intraperitoneal application of ketamine and midazolam. The abdomen was opened through a midline section, intestines moved upwards and the aorta and inferior vena cava were exposed in the retroperitoneum. Using 1.2 mm needle (Becton-Dickinson), the abdominal aorta was pierced into inferior vena cava between renal artery and bifurcation. The needle was removed after clamping the aorta above and applying acrylamide tissue glue to the puncture site. After 3 min, the clamp was removed and the functionality of the shunt was verified by pulsation of the inferior vena cava. Sham-operated rats underwent the same procedure without needle puncture.

Since the fistula have spontaneously closed in some operated animals, only rats with visually-verified fistula patency at the termination and heart to body weight (BW) ratio over 4 g/kg were used for quantitative morphological evaluation.

Morphological Examination

At 11 and 21 weeks after AVF procedure, rats were anesthetized with intraperitoneal phenobarbital application, sacrificed by exsanguination and their organs were weighted. Beating heart was excised and the coronary tree was immediately orthogradely perfused with 10 mL ice-cold St. Thomas cardioplegia solution. The hearts were fixed in 4% paraformaldehyde in phosphate buffer saline (PBS) and ran through ascending series of saccharose prior to embedding into Tissue-Tek. The blocks were cut on cryomicrotome at 12 μm thickness.

Guide series were stained by hematoxylin-eosin with alcian blue using usual techniques. Sister sections were stained by the following primary antibodies: cardiac α-actinin (monoclonal mouse antibody, Sigma, Clone EA-53, #A7811, 1:500), connexin43 (polyclonal rabbit antibody, Sigma, #C6219, 1:200), and phosphoconnexin43 (polyclonal rabbit antibody, Cell Signaling Technology, #3511, 1:100).

The staining was performed in dark humid chamber. On Day 1, the sections were blocked in normal goat serum (1:20) and in 1% bovine serum albumin in (PBS) for 20 min. Primary antibody was then applied overnight. On Day 2, the sections were washed in three changes of PBS, and species-appropriate secondary antibody conjugated with Rhodamine Red (Jackson Immuno Research) was applied for 4 hr in the dark. After washing in PBS again was applied solution of wheat germ agglutinin (WGA) conjugated with Alexa 488 (1:50, Invitrogen, #W11261) followed by three washes in PBS. WGA is a lectin, which binds to basal membranes and extracellular matrix and thus can be indirectly used also for detection of fibrosis. Finally, the nuclei were counterstained with Hoechst 33258 (1:100,000 diluted in 0.1% Triton-X in distilled water, Sigma-Aldrich, #86140-5). In the end, the sections were washed with distilled water and dehydrated in ascending series of ethanol (70%−100%), cleared in xylene, and mounted in Depex medium.

Western Blotting

Left ventricle samples from AVF and sham-operated animals (pools of six hearts per group) were pulverized under liquid nitrogen and extracted in NHT buffer (140 mM NaCl, 10 mM HEPES, 1.5% Triton X-100, pH 7.4) containing Phosphatase Inhibitor Cocktail 1 (Sigma-Aldrich, Czech Republic). Samples (40 μg) were combined with SDS loading buffer containing DTT, boiled for 5 min and resolved by SDS-PAGE on precast 4%−15% gradient minigels (Bio-Rad, CA) in Tris-Glycine buffer. Electrophoresis was performed in quadruplicate at constant voltage for 30 min at 45 V per gel, and then at 90 V per gel until the dye front reached the gel bottom. Proteins were then transferred to 0.45 μm PVDF membranes (Millipore, MA) in semi-dry blotter (Hoeffer, Canada) at 0.8 mA/cm^2 of membrane for 80 min. Membranes were incubated with blocking buffer containing PBS and 0.1% TWEEN 20 for 2 hr. As primary antibodies, rabbit anti-connexin (1:6,000, Sigma-Aldrich) and anti-phospho-connexin (1:1,000, Cell Signaling Technology) antibodies were used. After thorough washing in blocking buffer, secondary horseradish peroxidase-conjugated goat anti-rabbit antibody (1:16,000, Sigma-Aldrich) was applied for 1 hr. After washing, signal was detected using Western Blotting Luminol Reagent (Santa Cruz

Biotechnology, CA) and membranes were exposed to X-ray films (Kodak, Czech Republic). Membranes were scanned on GS-800 calibrated densitometer (Bio-RAD) and the signal was quantified by the Quantity One software (Bio-Rad).

Quantitative Evaluation and Statistical Analysis

The quantitative analysis is based upon numbers of animals indicated in Tables 1 and 2. In total, 14 AVF and 14 sham hearts were analyzed.

Image acquisition was performed on Leica SPE confocal microscope (immunofluorescence) and Olympus BX51 microscope with DP70 CCD camera (transmitted light). Six optical sections per each sample spaced by one micron were projected using maximum intensity algorithm. The images were analyzed using standard imaging software (Adobe Photoshop, ImageJ).

Myocyte width in midmyocardium and subendocardium was evaluated on sections stained with anti α-actinin antibody and WGA. Cell length and differences in connexin43 levels and distribution was evaluated on anti-connexin43 staining with WGA. For evaluation of phosphorylated connexin43 changes, we used specific phosphorylated connexin43 antibody. Fibrosis was evaluated using WGA staining and confirmed by Picrosirius Red staining examined in polarized light.

The cell width and length in midmyocardium was measured by averaging 10 cell transverse diameters from each confocal image. Cell width in papillary muscle was calculated from cross sectional areas of myocytes, assuming circular geometry, using also 10 cells from each image. To avoid underestimation, only cells in which nucleus was present were measured.

The distribution and localization of connexin43 and phosphorylated connexin43 was measured by comparing red channel (representing connexin43 or phosphorylated connexin43) and green channel (representing myocyte cytoplasmic autofluorescence) of confocal images using threshold and area measurements in ImageJ. The same procedure was used for evaluation of fibrosis on WGA pictures.

All data are presented as a mean ± SD. Differences between groups were statistically analyzed by unpaired Student's two-tailed t-test. Differences were considered statistically significant at a value of $P < 0.05$.

RESULTS

Organ Changes After AVF

We measured BW, weight of the whole heart, ventricles, and atria separately as well as weight of some other organs (lungs, liver, kidneys) on both sampling intervals. Changes in the whole animal BW were not significant (Table 1). The heart weight was considerably increased (by 96% after 11 weeks and by 140% after 21 weeks of volume overload). The contribution of individual chambers to total heart weight increase was also evaluated. In addition to heart weight increase, the changes can be better expressed by heart to BW ratio. This ratio was significantly increased at both stages, clearly demonstrating cardiac hypertrophy.

Concerning the other organs, the lungs were significantly heavier (by 26% after 11 weeks and by 61% after

TABLE 2. Quantification of cellular changes in the heart of AVF rats with heart failure

Changes in the heart	After 11 weeks				After 21 weeks			
	AVF (n = 7)	Sham (n = 6)	Difference	Statistics files *t*-test)	AVF (n = 7)	Sham (n = 8)	Difference	Statistics (*t*-test)
Wall thickness (mm)								
Left ventricle	29.99 ± 5.87	22.56 ± 3.00	+ 33%	$\boldsymbol{P = 0.020}$	46.02 ± 5.61	25.05 ± 1.53	+ 83.7%	$\boldsymbol{P = 3 \times 10^{-6}}$
Right ventricle	15.51 ± 1.76	9.81 ± 1.30	+ 58.1%	$\boldsymbol{P = 3 \times 10^{-4}}$	30.05 ± 4.44	12.23 ± 1.96	+ 146%	$\boldsymbol{P = 3 \times 10^{-6}}$
Myocyte size (Mm)								
Width in LV midmyocardium	11.03 ± 0.77	10.18 ± 0.82	+ 8.3%	$P = 0.083$	14.20 ± 2.62	9.78 ± 1.02	+ 45.1%	$\boldsymbol{P = 0.003}$
Width in LV papillary muscle	29.65 ± 4.57	24.96 ± 2.42	+ 18.8%	$P = 0.064$	28.87 ± 4.41	26.15 ± 3.52	+ 22.5%	$P = 0.249$
Length in LV midmyocardium	117.43 ± 8.07	62.26 ± 6.78	+ 88.6%	$\boldsymbol{P = 2 \times 10^{-7}}$	115.83 ± 14.97	58.77 ± 1.84	+ 97.0%	$\boldsymbol{P = 0.013}$
Width in RV midmyocardium	14.39 ± 0.86	10.14 ± 0.25	+ 42.0%	$\boldsymbol{P = 0.001}$	13.94 ± 1.71	10.43 ± 0.80	+ 33.6%	$\boldsymbol{P = 0.001}$
Length in RV midmyocardium	114.73 ± 6.92	85.73 ± 3.01	+ 33.8%	$\boldsymbol{P = 7 \times 10^{-5}}$	116.41 ± 5.26	89.65 ± 4.51	+ 29.8%	$\boldsymbol{P = 2 \times 10^{-4}}$

Data are presented as mean ± SD.

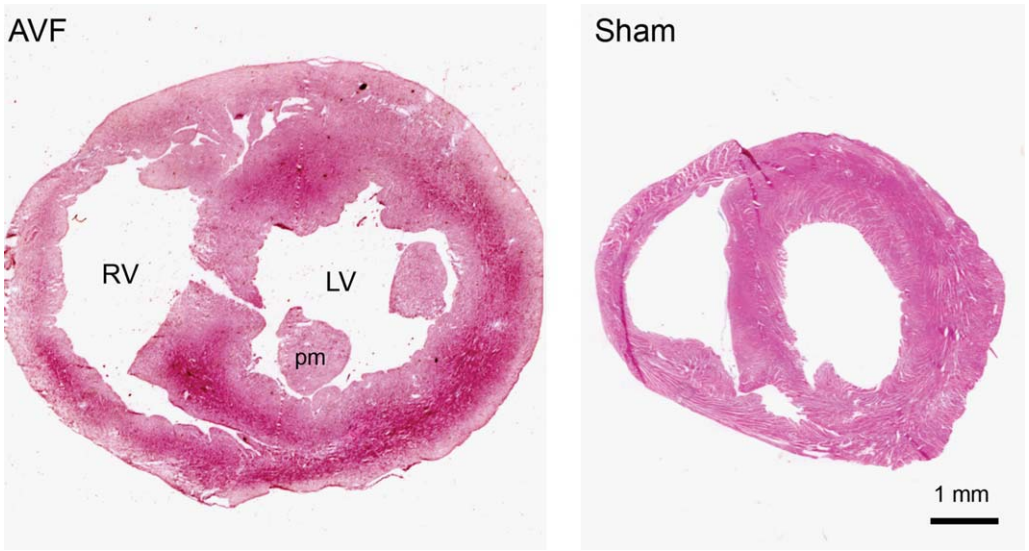

Fig. 1. Hematoxylin-eosin staining of frozen sections of AVF and sham-operated rat hearts. Note gross increase in heart size. LV, left ventricle, pm, papillary muscle, RV, right ventricle.

21 weeks of volume overload) which corresponds to development of HF and to congestion in the pulmonary circulation. Weight of liver and kidneys was not significantly changed.

Ventricular fibrosis was also evaluated from WGA confocal images and no significant changes were found. The ratio of green channel area (WGA staining, thus showing membranes and fibrotic tissues around myocytes) to area of all tissues on the section in AVF was 25.98% ± 6.27; and in controls 28.62% ± 3.87 ($P = 0.39$). This data was obtained from the hearts with decompensated HF (21 weeks after surgery), and confirmed by Picrosirius Red staining that showed likewise no differences between AVF and sham ventricles (data not shown).

Cellular Changes in the Ventricles

For understanding of morphological changes in the heart, we measured free wall thickness of the left and right ventricle (Fig. 1) and myocyte dimensions in the left ventricular myocardium (Table 2).

Both ventricles showed hypertrophy (Fig. 2) and its extent increased with time of volume overload, which can be clearly seen by the dynamics of wall thickness increase in both ventricles (Table 2). Right ventricle was more affected by volume overload from aortocaval shunt than the left ventricle (after 21 weeks of volume overload the left ventricle wall thickness increased by 84% vs. 146% for the right ventricle).

The thickness and the length of myocytes were measured on confocal images in midmyocardial layer of both ventricles and in the papillary muscle of the left ventricle. The hypertrophy in the midmyocardial layer was more extensive than in the subendocardium. The cells in the papillary muscles also underwent hypertrophy (Fig. 2) but the increase was smaller (by 19% after 11 weeks and by 23% after 21 weeks of volume overload, P = NS). The cell thickness in midmyocardial layer increased significantly (by 8% and 45%, respectively) in both ventricles with developing ventricular hypertrophy. Cell length in midmyocardium increased in both stages by 90% in the left ventricle and by 30% in the right ventricle, which indicates dilation of the ventricles (Table 2).

Connexin43 Expression

Using immunofluorescence staining and confocal microscopy imaging, we have qualitatively assessed total amount of connexin43 in myocytes, evaluated the distribution of connexin within the cells as well as the differences in phosphorylated isoform of connexin43. The measurements were performed in left ventricular myocardium 21 weeks after aortocaval fistula creation.

We found no notable difference in total amount of connexin43 per cell (Fig. 3). A small decrease could be seen in connexin43 levels during volume overload. The localization of connexin43 in the cell is an important determinant of possible arrhythmogenesis. We measured percentage of connexin43 in intercalated discs from the total amount of connexin43 in the cell (which can be localized also on the sides of cells and in the cytoplasm). We found no significant difference between AVF and sham-operated rats. AVF rats had 33.7% of connexin43 florescence situated in intercalated discs, sham-operated rats had 35.5% of connexin43 in the discs ($P = 0.8$).

Phosphorylation of connexin43 is important for functionality of this protein in gap junctions. We thus evaluated the amount of phosphorylated connexin43 in left ventricular myocardium on both stages and found that there was no apparent decrease in phosphorylated isoform of connexin43 in AVF group in the stage of compensated cardiac hypertrophy (11 weeks after creating the fistula). At the stage of decompensated HF (21 weeks after creating the fistula), however, the decrease in expression of the phosphorylated isoform was notable (Fig. 3).

The amount of total and phosphorylated connexin43 were quantified by western blotting on pools of 6 AVF

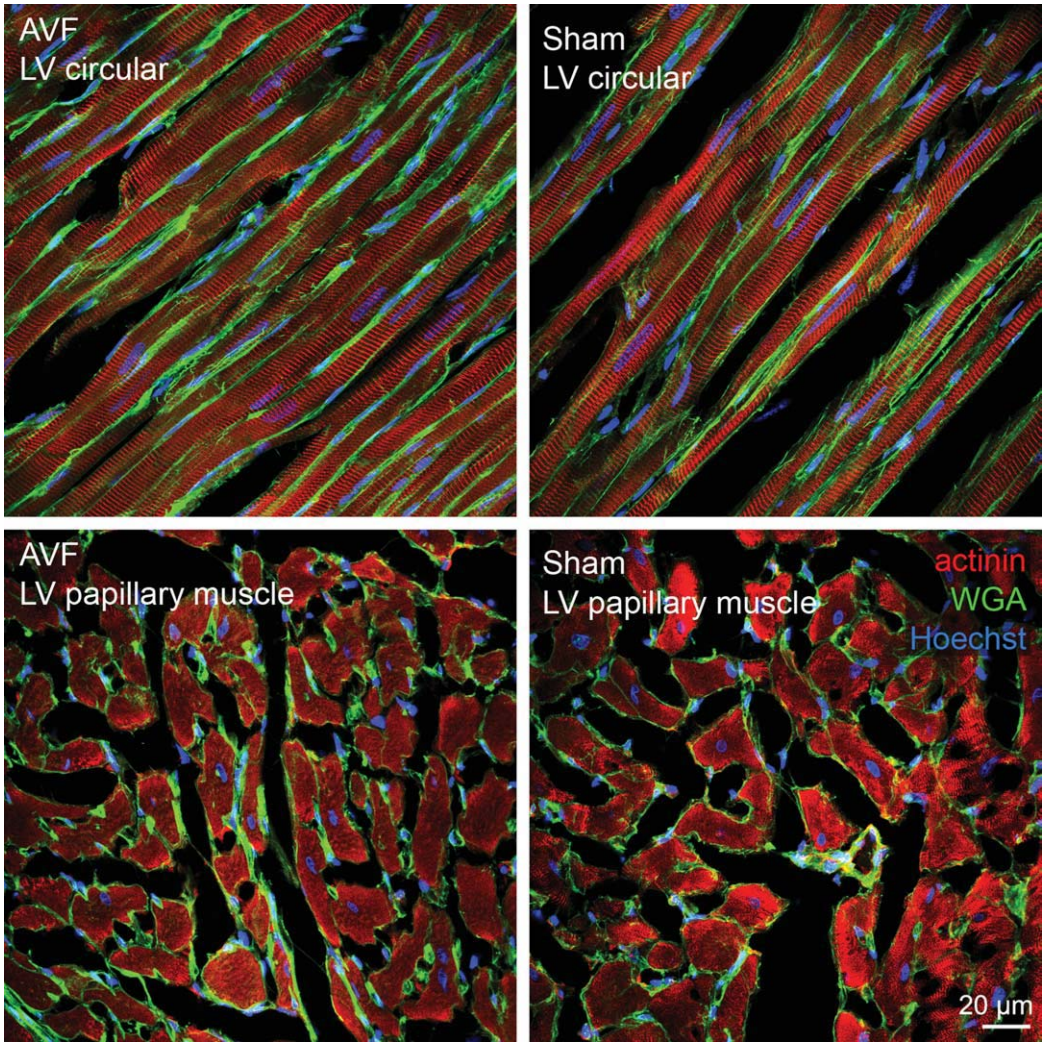

Fig. 2. Confocal micrographs of left ventricular midmyocardium (upper panels) and cross sections through papillary muscles of left ventricle (lower panels). Note increase in transverse myocyte diameter in the AVF hearts. For values of myocyte width please see Table 2. There is no increase in fibrosis (WGA, green staining).

and 6 sham samples at 21 weeks. There was over 60% decrease in both isoforms (Fig. 4).

DISCUSSION

Aortocaval fistula results in volume overload, which induces cardiac dilation and hypertrophy. Over time, this leads to HF and increased mortality. In our study, rats at 21 weeks demonstrated not only hypertrophy, but also decompensated HF phenotype with increased normalized weight of lungs and HF symptoms. In the failing rats, there was an increased heart weight, heart to BW ratio, and thickness of ventricular walls. The hypertrophy was present already after 11 weeks and the heart weight did not change with the time of volume overload, which shows that hypertrophy as a compensatory mechanism evolving early after creation of AVF. However, this compensated state became decompensated over time, resulting in development of congestive HF, as was demonstrated by increasing lung weight. The dynamic nature of changes during development of HF was best exemplified by increased heart to BW ratio, which was increased by almost 90% at 11 weeks but by more than 130% at 21 weeks in comparison with aged-matched sham controls (Table 1). Since the total weight of the animals did not change significantly, other organs have to shrink; this indicates increased catabolic state characteristic of HF and documented in a separate functional and metabolic study (Benes et al., submitted) by decreased fat reserves. At present, we are evaluating chronic changes in animals that have been in HF for 1 year to extend the longitudinal aspect of this study and to see the combined effects of HF and ageing. Cardiac dilation and hypertrophy were confirmed by increased size of cardiomyocytes, which were enlarged in both longitudinal and transverse diameters. Cardiomyocytes in

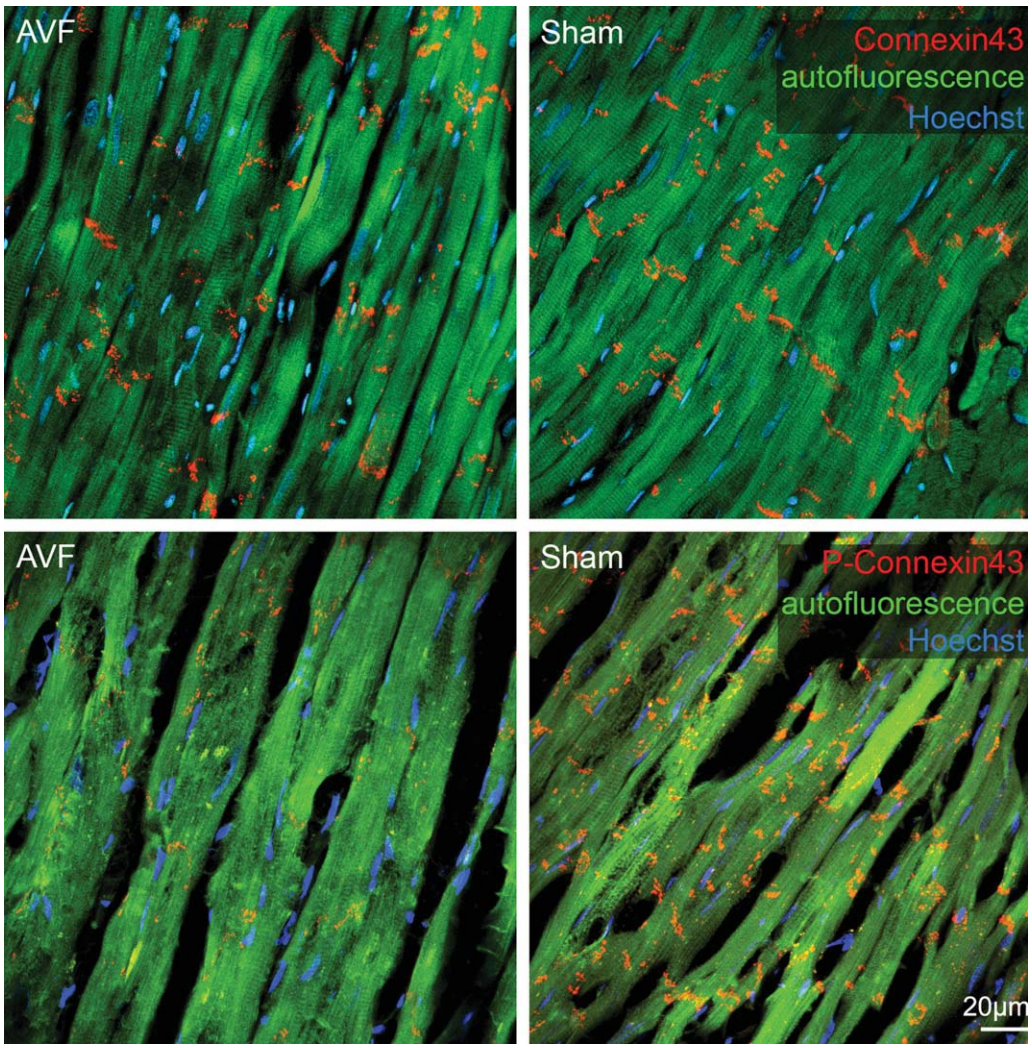

Fig. 3. Distribution and phosphorylation of connexin43 in left ventricular myocardium. Upper panels show confocal images of connexin43 distribution. Lower panels show confocal images of phosphoconnexin43 localization in left ventricular myocardium.

midmyocardium were more affected than those in papillary muscles. This is in contrast with asymmetric cellular hypertrophy in pressure overload model (Campbell et al., 1989), where most pronounced hypertrophy was found in the subendocardial layers. The interesting discrepancy between continued increase in ventricular wall thickness that could not be explained by increased myocyte dimensions, especially in the right ventricle (Table 2) suggests, in the notable absence of fibrosis, that there could be activation of myocyte (or resident stem cells) proliferation, that was recognized previously in decompensated HF in humans (Kajstura et al., 1998).

AVF model of volume overload induced HF had been described before. However, no previous study described these changes in decompensated HF stage. The principal new findings of our study include distinction between compensated (11 weeks) and decompensated (21 weeks) stage of HF, complete morphological evaluation of possible arrhythmogenic substrates (cell size and shape, connexin expression and distribution, fibrosis) and providing links between these findings and ventricular arrhythmias (Fig. 5). Our data thus provide solid morphological grounds for ongoing functional, metabolic and pharmacological studies in this model. Ruzicka et al. used this model for describing renin-angiotensin system and effects of angiotensin converting enzyme inhibitors in situation of volume overload (Ruzicka et al., 1993). Ryan et al. described remodeling process induced by bradykinin (Ryan et al., 2007). Study of Hatt et al. (1979) is closest to our morphological approach. Hatt et al. measured cells in failing hearts and our study generally corresponds with their findings. Their sampling intervals were 1 and 6 months, so it is not possible to compare exactly our findings with theirs. In their study, the hearts of rats with volume overload increased their weight by 81% after 6 month (compare to our increase by 140% after 21 weeks). They also measured cell width in midwall and in subendocardium and described greater increase in cell width in subendocardium than in midwall, which is in contrast to our data. Generally, the

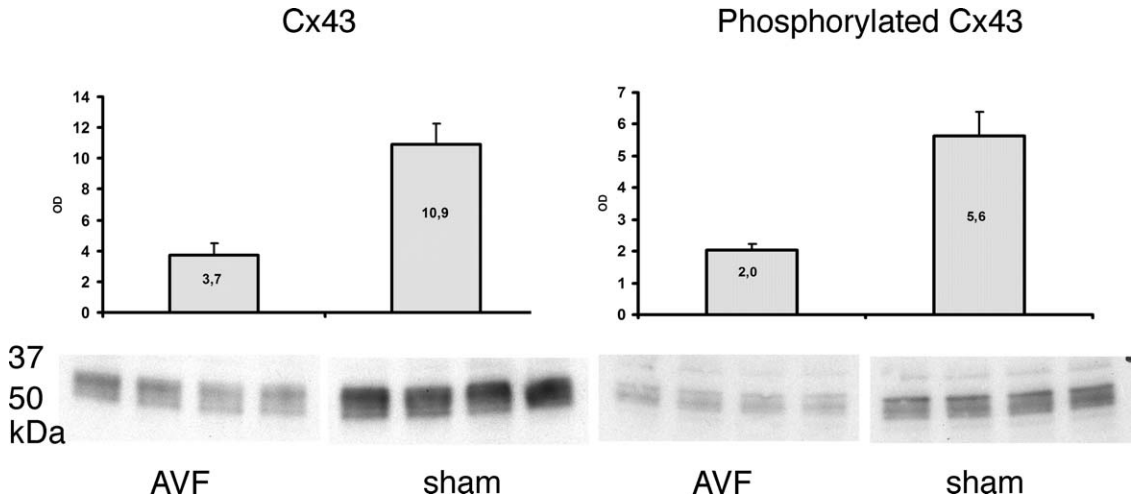

Fig. 4. Western blot on a pool of 6 + 6 samples performed in quadruplicate shows over 60% decrease in both total and phosphorylated connexin43 in the AVF hearts 21 weeks after shunt creation. Values are mean ± SD.

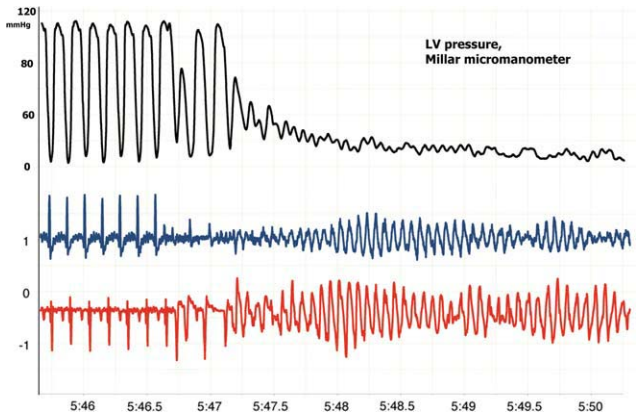

Fig. 5. ECG tracing (2 leads, bottom) and the left ventricular pressure tracing (2F Millar catheter) from a rat with AVF. Several ectopic beats degenerate into fast polymorphic ventricular tachycardia and later to ventricular fibrillation with immediate collapse of the circulation, visible in the pressure channel.

changes they described in the group of rats 6 month after performing the fistula were much milder than our findings. The possible reason for this is that they used female rats and there is known strong gender difference in cardiac response to volume overload—females are far less prone to eccentric remodeling and to the development of HF symptoms (Gardner et al., 2009). Since the methodology of fistula creation was not described in detail in that study, it is also possible that their method of fistula creation may have differed (e.g., different diameter of the needle, no exclusion of animals where AVF closed spontaneously). The reason for different findings in subendocardial myocyte width changes can be explained by the fact that we measured width in papillary muscle from transversal sections through the cells while Hatt et al. measured cells in myocardial wall in transversal sections.

Hypertrophic or failing rat or human hearts have bigger predisposition to develop severe ventricular arrhythmias (von Olshausen et al., 1983; Kligfield et al., 1987). Increased risk of sudden, presumably arrhythmic death was found even in asymptomatic subjects with left ventricular volume overload due to mitral regurgitation (Grigioni et al., 1999). Similarly, we observed increased excitability of hypertrophied AVF hearts, characterized by high frequency of ventricular ectopic beats and bursts of ventricular tachycardia, particularly during intraventricular measurements of pressure using Millar catheter (our unpublished observations). In several AVF animals, this ectopy even degenerated into lethal ventricular fibrillation, which is exceedingly rare in normal rat hearts (Fig. 5). In previous study that examined long-term survival of rats with AVF, 27% of all animals died without preceding HF symptoms (Brower and Janicki 2001), suggesting that arrhythmic sudden cardiac death occurs in substantial proportion of animals with AVF-induced chronic volume overload. Since no excessive collagen accumulation was found in the ventricular myocardium, we suggest that other arrhythmogenic mechanisms than fibrosis might be involved. In our study, we focused on connexin43 changes. Changes in connexin43 can lead to slowing of conduction velocity in ventricular wall, which may create a substrate for re-entry phenomenon (Libby et al., 2008). The main changes described in previous studies were changes in expression, localization, and phosphorylation (Severs et al., 2004). This is not, however, the only possible mechanism. Other contributing factors can be changes in ion channel expression, which can also substantially contribute to arrhythmogenesis (Shah et al., 2005).

In a partial contrast with previous studies of connexin43 changes in HF (Dupont et al., 2001; Emdad et al., 2001; Uzzaman et al., 2000), we found only mild difference in total connexin43 levels by immunohistochemistry (but there was over 60% reduction by Western blot), and the changes in localization were also insignificant. Possible reason for this discrepancy can be differences in HF models or methods used. Dupont et al. described the changes in humans and used Northern blot for quantification, detecting thus mRNA levels

(Dupont et al., 2001). Emdad et al. described HF in rats induced by pressure overload from aortic banding and they used enzymatic separation of myocytes to measure connexin43 levels by immunohistochemistry (Emdad et al., 2001). Recent study of Burstein et al. described changes in dog HF atria and they found also no difference in the amount of connexin43, which corresponds to our immunohistochemistry data (Burstein et al., 2009). Study of Goldfine et al. describes connexin43 changes in volume overload HF model. They found decrease in connexin43 levels in acute state of volume overload HF but when compensatory hypertrophy developed, the amount of connexin43 seemed to normalize (Goldfine et al., 1999). In any case, the absolute levels of connexin43 have to be decreased over 50% to induce significant physiological phenotype per se, as indicated by apparent normality of connexin43 heterozygous mice as well as ventricular arrhythmias leading to sudden cardiac death observed in myocardium-restricted null animals (Gutstein et al., 2001). In this respect, the 60% decreased in total amount of connexin43 found in our Western blot seems biologically sufficiently significant to form (together with changes in cell shape) a proarrhythmogenic substrate, as ventricular arrhythmias were recorded in ~10% of our HF animals.

Phosphorylation of connexin43 can influence conductance, assembly and degradation of gap junctions (Lampe and Lau, 2004; Laird, 2005; Solan and Lampe, 2005). Recent work suggests an important role of connexin43 phosphorylation in HF (Akar et al., 2004; Ai and Pogwizd, 2005). We found greatly decreased phosphorylation of connexin43 in the stage of decompensated HF (21 weeks after operation). The phosphorylation of connexin43 at the earlier stage, when congestive HF was not yet developed (11 weeks after operation), was also slightly decreased but without statistical significance. Thus, our data suggest that the HF and not the hypertrophy itself contribute to the hypophosphorylation. Targeting the phosphorylation status of connexin43 using specific drugs in patients with HF can be a method to prevent development of fatal ventricular arrhythmias.

ACKNOWLEDGMENTS

We would like to express our sincere thanks to Ms. Eva Kluzakova and Ms. Marie Jindrakova for their excellent technical assistance. D. Sedmera is a recipient of the Purkinje Fellowship from the Academy of Sciences of the Czech Republic.

LITERATURE CITED

Ai X, Pogwizd SM. 2005. Connexin 43 downregulation and dephosphorylation in nonischemic heart failure is associated with enhanced colocalized protein phosphatase type 2A. Circ Res 96: 54–63.

Akar FG, Spragg DD, Tunin RS, Kass DA, Tomaselli GF. 2004. Mechanisms underlying conduction slowing and arrhythmogenesis in nonischemic dilated cardiomyopathy. Circ Res 95:717–725.

Artham SM, Lavie CJ, Milani RV, Patel DA, Verma A, Ventura HO. 2009. Clinical impact of left ventricular hypertrophy and implications for regression. Prog Cardiovasc Dis 52:153–167.

Beardslee MA, Lerner DL, Tadros PN, Laing JG, Beyer EC, Yamada KA, Kleber AG, Schuessler RB, Saffitz JE. 2000. Dephosphorylation and intracellular redistribution of ventricular connexin43 during electrical uncoupling induced by ischemia. Circ Res 87:656–662.

Brower GL, Janicki JS. 2001. Contribution of ventricular remodeling to pathogenesis of heart failure in rats. Am J Physiol Heart Circ Physiol 280:H674–H683.

Burstein B, Comtois P, Michael G, Nishida K, Villeneuve L, Yeh YH, Nattel S. 2009. Changes in connexin expression and the atrial fibrillation substrate in congestive heart failure. Circ Res 105:1213–1222.

Campbell SE, Rakusan K, Gerdes AM. 1989. Change in cardiac myocyte size distribution in aortic-constricted neonatal rats. Basic Res Cardiol 84:247–258.

Dupont E, Matsushita T, Kaba RA, Vozzi C, Coppen SR, Khan N, Kaprielian R, Yacoub MH, Severs NJ. 2001. Altered connexin expression in human congestive heart failure. J Mol Cell Cardiol 33:359–371.

Emdad L, Uzzaman M, Takagishi Y, Honjo H, Uchida T, Severs NJ, Kodama I, Murata Y. 2001. Gap junction remodeling in hypertrophied left ventricles of aortic-banded rats: prevention by angiotensin II type 1 receptor blockade. J Mol Cell Cardiol 33:219–231.

Ford LE. 1976. Heart size. Circ Res 39:297–303.

Garcia R, Diebold S. 1990. Simple, rapid, and effective method of producing aortocaval shunts in the rat. Cardiovasc Res 24:430–432.

Gardner JD, Murray DB, Voloshenyuk TG, Brower GL, Bradley JM, Janicki JS. 2010. Estrogen Attenuates Chronic Volume Overload Induced Structural and Functional Remodeling in Male Rat Hearts. Am J Physiol Heart Circ Physiol 298:H497–H504.

Goldfine SM, Walcott B, Brink PR, Magid NM, Borer JS. 1999. Myocardial connexin43 expression in left ventricular hypertrophy resulting from aortic regurgitation. Cardiovasc Pathol 8:1–6.

Grigioni F, Enriquez-Sarano M, Ling LH, Bailey KR, Seward JB, Tajik AJ, Frye RL. 1999. Sudden death in mitral regurgitation due to flail leaflet. J Am Coll Cardiol 34:2078–2085.

Grossman W, Jones D, McLaurin LP. 1975. Wall stress and patterns of hypertrophy in the human left ventricle. J Clin Invest 56:56–64.

Gutstein DE, Morley GE, Tamaddon H, Vaidya D, Schneider MD, Chen J, Chien KR, Stuhlmann H, Fishman GI. 2001. Conduction slowing and sudden arrhythmic death in mice with cardiac-restricted inactivation of connexin43. Circ Res 88:333–339.

Haider AW, Larson MG, Benjamin EJ, Levy D. 1998. Increased left ventricular mass and hypertrophy are associated with increased risk for sudden death. J Am Coll Cardiol 32:1454–1459.

Hatt PY, Rakusan K, Gastineau P, Laplace M. 1979. Morphometry and ultrastructure of heart hypertrophy induced by chronic volume overload (aorto-caval fistula in the rat). J Mol Cell Cardiol 11:989–998.

Haugan K, Miyamoto T, Takeishi Y, Kubota I, Nakayama J, Shimojo H, Hirose M. 2006. Rotigaptide (ZP123) improves atrial conduction slowing in chronic volume overload-induced dilated atria. Basic Clin Pharmacol Toxicol 99:71–79.

Hood WP, Jr., Rackley CE, Rolett EL. 1968. Wall stress in the normal and hypertrophied human left ventricle. Am J Cardiol 22:550–558.

Kajstura J, Leri A, Finato N, Di Loreto C, Beltrami CA, Anversa P. 1998. Myocyte proliferation in end-stage cardiac failure in humans. Proc Natl Acad Sci U S A 95:8801–8805.

Kligfield P, Hochreiter C, Niles N, Devereux RB, Borer JS. 1987. Relation of sudden death in pure mitral regurgitation, with and without mitral valve prolapse, to repetitive ventricular arrhythmias and right and left ventricular ejection fractions. Am J Cardiol 60:397–399.

Kostin S, Rieger M, Dammer S, Hein S, Richter M, Klovekorn WP, Bauer EP, Schaper J. 2003. Gap junction remodeling and altered connexin43 expression in the failing human heart. Mol Cell Biochem 242:135–144.

Laird DW. 2005. Connexin phosphorylation as a regulatory event linked to gap junction internalization and degradation. Biochim Biophys Acta 1711:172–182.

Lampe PD, Lau AF. 2004. The effects of connexin phosphorylation on gap junctional communication. Int J Biochem Cell Biol 36:1171–1186.

Legault F, Rouleau JL, Juneau C, Rose C, Rakusan K. 1990. Functional and morphological characteristics of compensated and decompensated cardiac hypertrophy in dogs with chronic infrarenal aorto-caval fistulas. Circ Res 66:846–859.

Libby P, Bonow RO, Mann DL, Zipes DP, Braunwald E, editors. 2008. Braunwald's Heart Disease, 8th ed. Philadelphia: Elsevier.

Ruzicka M, Yuan B, Harmsen E, Leenen FH. 1993. The renin-angiotensin system and volume overload-induced cardiac hypertrophy in rats. Effects of angiotensin converting enzyme inhibitor versus angiotensin II receptor blocker. Circulation 87:921–930.

Ryan TD, Rothstein EC, Aban I, Tallaj JA, Husain A, Lucchesi PA, Dell'Italia LJ. 2007. Left ventricular eccentric remodeling and matrix loss are mediated by bradykinin and precede cardiomyocyte elongation in rats with volume overload. J Am Coll Cardiol 49:811–821.

Severs NJ, Coppen SR, Dupont E, Yeh HI, Ko YS, Matsushita T. 2004. Gap junction alterations in human cardiac disease. Cardiovasc Res 62:368–377.

Shah M, Akar FG, Tomaselli GF. 2005. Molecular basis of arrhythmias. Circulation 112:2517–2529.

Sohl G, Willecke K. 2004. Gap junctions and the connexin protein family. Cardiovasc Res 62:228–232.

Solan JL, Lampe PD. 2005. Connexin phosphorylation as a regulatory event linked to gap junction channel assembly. Biochim Biophys Acta 1711:154–163.

Uzzaman M, Honjo H, Takagishi Y, Emdad L, Magee AI, Severs NJ, Kodama I. 2000. Remodeling of gap junctional coupling in hypertrophied right ventricles of rats with monocrotaline-induced pulmonary hypertension. Circ Res 86:871–878.

von Olshausen K, Schwarz F, Apfelbach J, Rohrig N, Kramer B, Kubler W. 1983. Determinants of the incidence and severity of ventricular arrhythmias in aortic valve disease. Am J Cardiol 51:1103–1109.

Wiegerinck RF, van Veen TA, Belterman CN, Schumacher CA, Noorman M, de Bakker JM, Coronel R. 2008. Transmural dispersion of refractoriness and conduction velocity is associated with heterogeneously reduced connexin43 in a rabbit model of heart failure. Heart Rhythm 5:1178–1185.